Journal of Contaminant Hydrology 197 (2017) 50–61

Contents lists available at ScienceDirect

Journal of Contaminant Hydrology

journal homepage: www.elsevier.com/locate/jconhyd

Analytical model for the design of in situ horizontal permeable reactive barriers (HPRBs) for the mitigation of chlorinated solvent vapors in the unsaturated zone

Iason Verginelli [a], Oriana Capobianco [a], Niels Hartog [b,c], Renato Baciocchi [a,*]

[a] Laboratory of Environmental Engineering, Department of Civil Engineering and Computer Science Engineering, University of Rome "Tor Vergata", Rome, Italy
[b] KWR Watercycle Research Institute, Nieuwegein, The Netherlands
[c] Utrecht University, Department of Earth Sciences, The Netherlands

ARTICLE INFO

Article history:
Received 23 June 2016
Received in revised form 2 November 2016
Accepted 25 December 2016
Available online 10 January 2017

Keywords:
Permeable reactive layer
Vapor mitigation system
Chlorinated solvents
Potassium permanganate
Analytical model

ABSTRACT

In this work we introduce a 1-D analytical solution that can be used for the design of horizontal permeable reactive barriers (HPRBs) as a vapor mitigation system at sites contaminated by chlorinated solvents. The developed model incorporates a transient diffusion-dominated transport with a second-order reaction rate constant. Furthermore, the model accounts for the HPRB lifetime as a function of the oxidant consumption by reaction with upward vapors and its progressive dissolution and leaching by infiltrating water. Simulation results by this new model closely replicate previous lab-scale tests carried out on trichloroethylene (TCE) using a HPRB containing a mixture of potassium permanganate, water and sand. In view of field applications, design criteria, in terms of the minimum HPRB thickness required to attenuate vapors at acceptable risk-based levels and the expected HPRB lifetime, are determined from site-specific conditions such as vapor source concentration, water infiltration rate and HPRB mixture. The results clearly show the field-scale feasibility of this alternative vapor mitigation system for the treatment of chlorinated solvents. Depending on the oxidation kinetic of the target contaminant, a 1 m thick HPRB can ensure an attenuation of vapor concentrations of orders of magnitude up to 20 years, even for vapor source concentrations up to 10 g/m^3. A demonstrative application for representative contaminated site conditions also shows the feasibility of this mitigation system from an economical point of view with capital costs potentially somewhat lower than those of other remediation options, such as soil vapor extraction systems. Overall, based on the experimental and theoretical evaluation thus far, field-scale tests are warranted to verify the potential and cost-effectiveness of HPRBs for vapor mitigation control under various conditions of application.

1. Introduction

Contamination of the subsurface by volatile organic compounds (VOCs) may cause vapor intrusion (VI), a process by which vapors diffuse into overlying buildings through cracks or other openings present in foundation slabs and basement walls (Eklund et al., 2012). The air quality problem resulting from VOCs vapors may pose potential threats to safety and possible adverse human health effects (McHugh et al., 2010).

Chlorinated hydrocarbons (CHCs) and petroleum hydrocarbons (PHCs) are the main volatile organic compounds that cause soil and groundwater contamination, due to their widespread production and use as organic solvents and fuels, respectively (Rivett et al., 2011). However, the risk of PHCs vapor intrusion may be drastically reduced in oxygen-rich soils due to the occurrence of relatively rapid aerobic biodegradation processes in the subsurface by ubiquitous soil microbes (Fischer et al., 1996; Hers et al., 2000; Patterson and Davis, 2009; Lahvis et al., 2013; Verginelli and Baciocchi, 2014; Yao et al., 2015, 2016; Verginelli et al., 2016a, b). Conversely, chlorinated solvents, such as tetrachloroethene (PCE), trichloroethene (TCE), dichloroethene (DCE) and vinyl chloride (VC), are considerably less susceptible to biodegradation. This makes VI a key issue in many sites contaminated by chlorinated solvents (McHugh et al., 2010). The conventional approach to avoid vapor intrusion of these compounds from contaminated soil or groundwater relies on the remediation of the subsurface soil to acceptable risk-based levels (U.S.EPA, 2015a), using one of the several cleanup technologies commercially available.

Often, in combination with site remediation approaches, different strategies can be designed to mitigate vapor intrusion risks. Methods for VI mitigation include the use of sub-slab depressurization systems by using fans or blowers installed below the building foundation, the over-pressurization of non-residential buildings by adjusting the heating, ventilating and air conditioning (HVAC) system, the enhancement of building ventilation using fans or natural ventilation, the sealing

* Corresponding author.
E-mail addresses: verginelli@ing.uniroma2.it (I. Verginelli), baciocchi@ing.uniroma2.it (R. Baciocchi).

http://dx.doi.org/10.1016/j.jconhyd.2016.12.010
0169-7722/

of cracks and openings in foundations and walls with bituminous products or elastomeric polymers and the installation of passive barriers below the building to physically block vapors access (ITRC, 2007; U.S.EPA, 2015a).

An alternative VI mitigation system involves the use of solid potassium permanganate to create a horizontal permeable reactive barrier (HPRB) aimed at oxidizing upward VOCs. In a series of batch and lab-scale column tests, Mahmoodlu et al. (2014a, b, 2015) have demonstrated the potential of HPRB in oxidizing TCE, toluene, and ethanol vapors migrating upward from a contaminated saturated zone. To scale-up these results and to evaluate the feasibility of this alternative mitigation system in real-scale applications, this study introduces a 1-D analytical solution that describes the attenuation of vapors through the reactive barrier. After a brief description of the analytical solution method, the developed model is compared with the results of the lab-scale column tests obtained by Mahmoodlu et al. (2015). Then, the simulation results provided by the model are used to suggest design criteria for permanganate HPRB in view of field applications. Specifically, the model outputs are used to evaluate the minimum HPRB thickness required to attenuate vapors at acceptable risk-based levels as a function of the vapor source concentration. Furthermore, the HPRB lifetime as a function of permanganate consumption due to oxidation and its progressive dissolution under conditions of net recharge is investigated. Finally, a field case study illustrating the potential applicability of HPRBs is presented. Beyond the prime focus on the use of HPRBs using solid potassium permanganate, the analytical approach presented in this work is applicable for the use of other reactive (sorbing or oxidizing) media to create HPRBs in the control of VOC migration in the unsaturated zone.

2. Model development

2.1. Vapor transport

2.1.1. Vapor attenuation through the reactive barrier

The governing equation for contaminant reactive transport (1-D along z direction) through the HPRB can be written, assuming a diffusion-dominated transport and a second-order reaction kinetic model for the oxidation of contaminant (Fig. 1), as follows:

$$\frac{\partial C_v}{\partial t} = D_{HPRB}\frac{\partial^2 C_v}{\partial z^2} - k''\frac{\theta_{w,HPRB}}{H}\cdot C_{ox}\cdot C_v \tag{1}$$

where C_v is the concentration of the contaminant in the soil-gas phase, C_{ox} the concentration of the oxidant in the water phase, t the time, k'' the second-order oxidation rate constant in the water phase, $\theta_{w,HPRB}$ the water-filled porosity in the HPRB, H the dimensionless Henry's law constant of the contaminant and D_{HPRB} the effective porous medium diffusion coefficient through the HPRB which can be estimated by using the Millington and Quirk (1961) equation:

$$D_{HPRB} = D_a\cdot\frac{\theta_{a,HPRB}^{10/3}}{\theta_{e,HPRB}^{2}} \tag{2}$$

where D_a is the diffusion coefficients of the contaminant in air, $\theta_{e,HPRB}$ the effective porosity in the HPRB and $\theta_{a,HPRB}$ the air-filled porosity in the HPRB.

When the oxidant availability in the HPRB is in such excess that it can be considered constant during the oxidation reaction, C_{ox} can be assumed equal to the solubility value of the oxidant (Hartog et al., 2015). This condition is indeed likely representative of the scenario modeled in this work as the reactant (i.e. permanganate) in the barrier is considered stoichiometrically in excess with respect to the contaminants migrating through the barrier.

An analytical solution of Eq. (1) can be obtained assuming as boundary conditions a vapor concentration entering the HPRB barrier equal to $C_{HPRB,in}$ (t) and a negligible vapor flux leaving the reactive layer of thickness d_{HPRB} (i.e. a complete attenuation of vapors through the barrier is assumed at $z = d_{HPRB}$) while as initial condition a contaminant concentration equal to zero within the whole HPRB barrier:

$$\begin{aligned} &C_v(0,t) = C_{HPRB,in}(t)\\ &C_v(z,0) = 0\\ &\frac{\partial C_v}{\partial z}(d_{HPRB},t) = 0 \end{aligned} \tag{3}$$

Note that the boundary condition on the vapor flux may lead to overestimate the attenuation of vapors expected through the reactive layer in the case of low oxidation rate constants and low HPRB thicknesses, since the assumption of a negligible vapor flux leaving the HPRB with respect to the one entering at the bottom of the reactive layer is no longer valid.

Assuming the initial and boundary conditions discussed above and summarized in Eq. (3), the following analytical solution is obtained:

$$C_v(z,t) = 0.5\cdot C_{HPRB,in}(t)\cdot\ \exp\left(-\frac{z}{L_R}\right)erfc\left(\frac{z}{2\omega}-\frac{\omega}{L_R}\right) \tag{4}$$

with

$$\omega = (D_{HPRB}\cdot t)^{1/2} \tag{5}$$

$$L_R = \left(\frac{D_{HPRB}\cdot H}{k''\cdot C_{ox}\cdot\theta_{w,HPRB}}\right)^{1/2} \tag{6}$$

Note that Eq. (4) represents a simplified form of the analytical solution reported by van Genuchten (1981).

At steady-state (i.e. assuming $t\to\infty$ in Eq. (4)), the vapor attenuation in the reactive barrier can be estimated as:

$$\frac{C_v(z,t\to\infty)}{C_{HPRB,in}(t\to\infty)} = \exp\left(-\frac{z}{L_R}\right) \tag{7}$$

At $z = d_{HPRB}$, Eq. (7) provides the attenuation factor of vapors, α, through the HPRB. Namely, at steady-state the attenuation of vapors through the HPRB depends only on the thickness of the barrier, d_{HPRB}, and on the extension of the diffusive reaction length, L_R, that can be calculated as in Eq. (6).

Eq. (7) can be rearranged to estimate the minimum thickness of the HPRB, d_{HPRB}^{*}, needed to attenuate vapors to acceptable risk-based levels:

$$d_{HPRB}{}^{*} = L_R\ \ln\left(\frac{C_{HPRB,in}}{C_{target}}\right) \tag{8}$$

where L_R is the diffusive reaction length and C_{target} the acceptable risk-based soil-gas concentration (for outdoor or indoor volatilization).

On the other hand, from Eq. (7) the flux of vapors through the HPRB layer can be estimated as follows:

$$J_{HPRB,layer}(z) = C_{HPRB,in}\cdot\frac{D_{HPRB}}{L_R}\cdot\ \exp\left(-\frac{z}{L_R}\right) \tag{9}$$

At the bottom of the HPRB layer, Eq. (9) becomes:

$$J_{HPRB,layer}(0) = C_{HPRB,in}\cdot\frac{D_{HPRB}}{L_R} \tag{10}$$

2.1.2. Estimation of the vapor concentrations entering the reactive layer

The governing equation for upward contaminant vapor transport (1-D along z direction) through the soil below the HPRB can be written

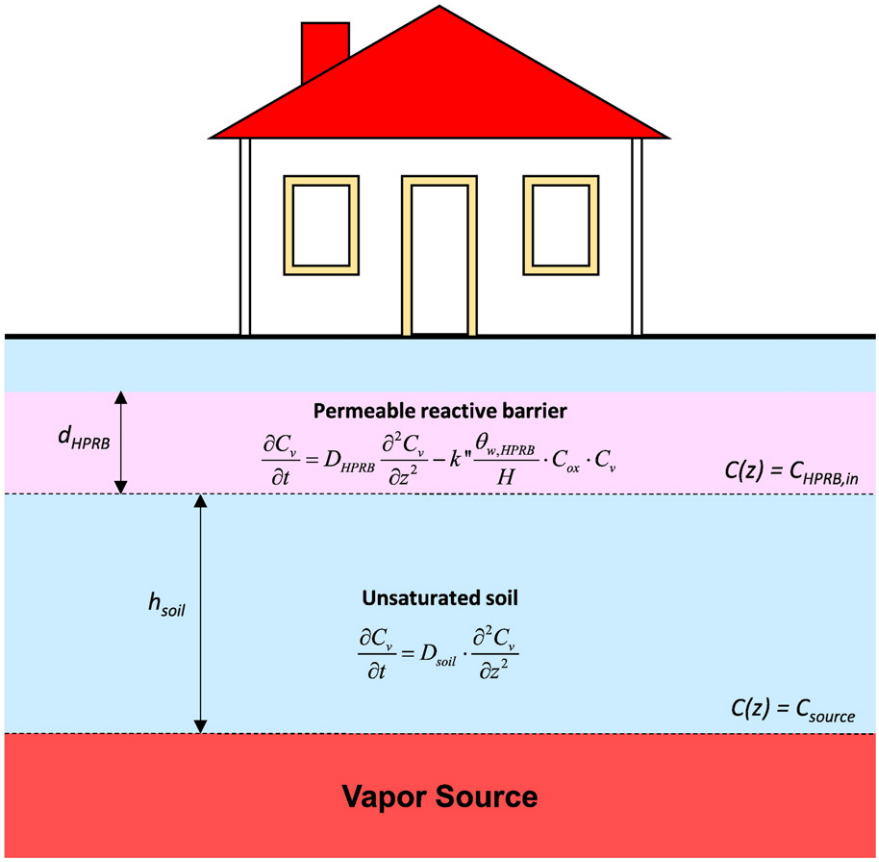

Fig. 1. Conceptual modeling scenario.

assuming a diffusion-dominated transport as follows:

$$\frac{\partial C_v}{\partial t} = D_{soil}\cdot\frac{\partial^2 C_v}{\partial z^2} \tag{11}$$

where D_{soil} is the effective porous medium diffusion coefficient of vapors through the soil that can be calculated with Eq. (2) using the air-filled porosity, $\theta_{a,soil}$, and the effective porosity, $\theta_{e,soil}$, of the soil. Note that for layered soils or to account for the vertical moisture profile in the soil, the effective diffusion coefficients, D_{soil}, can be calculated using the harmonic averaging method reported by Johnson et al. (1998).

An analytical solution of Eq. (11) can be obtained assuming a constant vapor concentration at the source, C_{source}, and an initial negligible concentration in the whole soil column below the HPRB:

$$\begin{aligned} C_v(0,t) &= C_{source} \\ C_v(z,0) &= 0 \end{aligned} \tag{12}$$

Assuming these boundary and initial conditions, reported in Eq. (12), the following analytical solution for the soil gas concentration entering the HPRB layer is obtained (Crank, 1975):

$$C_{HPRB,in}(t) = C_{source}\cdot erfc\left(\frac{h_{soil}}{2\cdot(D_{soil}\cdot t)^{1/2}}\right) \tag{13}$$

where h_{soil} is the vertical source to HPRB layer distance.

2.2. HPRB lifetime

2.2.1. HPRB depletion due to oxidation

Assuming that VOCs are completely oxidized in the HPRB, the lifetime of the reactive layer, $t^{*}_{HPRB,ox}$, can be calculated by stoichiometrically equating the mass of the oxidant present in the reactive layer with the mass of the stoichiometric oxidant consumption rate needed to oxidize the VOCs entering into the barrier:

$$t_{HPRB,ox}{}^{*} = \frac{M_{oxidant}}{\sum_{i=1}^{n}\gamma_i\cdot J_{HPRB,layer,i}(0)\cdot A_{HPRB}} \tag{14}$$

where γ is the stoichiometric mass ratio between the oxidant and the contaminant of concern, A_{HPRB} the horizontal surface area of the reactive layer and $M_{oxidant}$ the mass of oxidant in the reactive layer that can be calculated as:

$$M_{oxidant} = \rho_{HPRB}\cdot d_{HPRB}\cdot A_{HPRB}\cdot\eta \tag{15}$$

where ρ_{HPRB} is the bulk density of the reactive layer and η the mass fraction of the oxidant in the reactive layer, which can be estimated from Eqs. (16) and (17), respectively:

$$\rho_{HPRB} = \frac{M_{sand}+M_{oxidant}}{\left(\frac{M_{sand}}{\rho_{sand}}+\frac{M_{oxidant}}{\rho_{oxidant}}\right)\left(\frac{1}{1-\theta_e}\right)} \tag{16}$$

$$\eta = \frac{M_{oxidant}}{M_{oxidant}+M_{sand}} \tag{17}$$

with M_{sand} being the mass of sand in the HPRB, ρ_{sand} the particle density of the sand and $\rho_{oxidant}$ the particle density of the oxidant constituting the HPRB.

Hence, substituting Eqs. (15) and (10) into Eq. (14), the lifetime of the reactive layer due to oxidation, $t_{HPRB,ox}^{*}$, can be calculated as follows:

$$t_{HPRB,ox}^{*} = \frac{\rho_{HPRB} \cdot d_{HPRB} \cdot \eta}{\sum_{i=1}^{n} \gamma_i \cdot C_{HPRB,in,i} \cdot \frac{D_{HPRB,i}}{L_{R,i}}} \quad (18)$$

2.2.2. HPRB depletion due to leaching

Besides being reduced by the reaction with the contaminants in the vapor flux, the reactive capacity of the HPRB can be also depleted by leaching of the oxidant from infiltrating water. The relevance of the latter process will depend on the water solubility of the reactive media used as well as on the extent of water infiltration (e.g. subslab vs. open field application). For a HPRB with water soluble reactive media, such as potassium permanganate, the change of the mass source over time due to infiltrating water can be described by the mass balance reported by Verginelli and Baciocchi (2013):

$$-\frac{dM_{oxidant}}{dt} = I_{ef} \cdot A_{HPRB} \cdot S_{ox} \quad (19)$$

where S_{ox} is the oxidant solubility, A_{HPRB} the horizontal surface area of the reactive layer and I_{ef} the infiltration rate through the HPRB. Naturally, the oxidant leached from the HPRB may still oxidize contaminants either in the unsaturated or the saturated zone underlying the barrier, thus contributing to a reduction of the vapor source concentration.

Hence integrating Eq. (19), the oxidant mass over time due to leaching can be calculated as follows:

$$M_{oxidant}(t) = M_{oxidant}(t=0) - I_{ef} \cdot A_{HPRB} \cdot S_{ox} \cdot t \quad (20)$$

The lifetime of the reactive layer, i.e. the time corresponding to a complete depletion of the reactive layer by leaching, $t_{HPRB,leach}^{*}$, can be calculated by rearranging Eq. (20) and assuming $M_{oxidant}(t) = 0$:

$$t_{HPRB,leach}^{*} = \frac{M_{oxidant}}{I_{ef} \cdot A_{HPRB} \cdot S_{ox}} = \frac{\rho_{HPRB} \cdot d_{HPRB} \cdot \eta}{I_{ef} \cdot S_{ox}} \quad (21)$$

If no other data are available, the infiltration rate I_{ef} can be calculated using the following empirical equation (Connor et al., 1997):

$$I_{ef} = \beta \cdot P^2 \quad (22)$$

where P is the rainfall rate (cm/year) and β an empirical factor, whose values depend on the soil texture. For instance, Connor et al. (1997) report β values equal to 0.0018 for sandy soils (sand, loamy sand and sandy loam), 0.0009 for silty soils (sandy clay loam, loam, silt loam and silt) and 0.00018 for clay soils (clay loam, silty clay loam, silty clay, sandy clay and clay).

2.2.3. HPRB timeframe at high-level performance

As discussed above, the HRPB lifetime is limited by the consumption of the oxidant due to the reaction with contaminants in the vapor flux and by its leaching due to water infiltration. The overall lifetime of HPRB, t_{HPRB}^{*}, can be then estimated coupling Eqs. (18) and (21):

$$t_{HPRB}^{*} = \frac{\rho_{HPRB} \cdot d_{HPRB} \cdot \eta}{I_{ef} \cdot S_{ox} + \sum_{i=1}^{n} \gamma_i \cdot C_{HPRB,in,i} \cdot \frac{D_{HPRB,i}}{L_{R,i}}} \quad (23)$$

The HPRB lifetime calculated with Eq. (23) represents the time after which the complete depletion of the reactive layer occurs. Nevertheless, the effectiveness of the reactive layer in attenuating the vapor flux will be reduced well before its complete depletion, as a result of the progressive reduction with time of the layer thickness effectively available to oxidize the vapors.

In this sense, the design of the barrier could be carried out by fixing a timeframe, $t_{HPRB,desired}$, for which the mitigation system must continue to be effective in oxidizing the vapors (e.g. 10 years). Then this timeframe can be used in Eq. (24) to estimate the overdesign of the HPRB thickness, Δd_{HPRB}, needed to guarantee the effectiveness of the HPRB to attenuate VOCs at acceptable risk-based levels:

$$\Delta d_{HPRB} = \frac{\left(I_{ef} \cdot S_{ox} + \sum_{i=1}^{n} \gamma_i \cdot C_{HPRB,in,i} \cdot \frac{D_{HPRB,i}}{L_{R,i}}\right) \cdot t_{HPRB,desired}}{\rho_{HPRB} \cdot \eta} \quad (24)$$

Hence the thickness of HPRB for in situ applications (d_{HPRB}) can be calculated by adding the overdesign thickness (Δd_{HPRB} from Eq. (24)) to the minimum thickness needed to guarantee acceptable risk-based levels (d_{HPRB}^{*} from Eq. (8)):

$$d_{HPRB} = d_{HPRB}^{*} + \Delta d_{HPRB} \quad (25)$$

2.2.4. Estimation of diffusive reaction lengths and stoichiometric mass coefficients

The diffusive reaction length can be estimated by Eq. (6) once that the second-order rate oxidation constants (k''), the chemico-physical properties of the compound of concern and the oxidant concentration in the water phase are set. Making reference to chlorinated solvents of concern typically detected at contaminated sites, Table 1 reports the diffusive reaction lengths (L_R) for potassium permanganate, calculated applying Eq. (6), based on the second-order rate oxidation constants available in the recent literature for $KMnO_4$. Namely, the higher values of L_R in Table 1 correspond to the lower bound values of the k'' literature values, while the lower L_R to the higher k'' values reported in the table. For the estimation of L_R values, the concentration of the oxidant in the barrier was assumed equal to the solubility of potassium permanganate at 20 °C, i.e. 64 g/l (Mahmoodlu et al., 2014a). Furthermore, a relative water saturation, S^w ($S^w = \theta_{w,HPRB} / \theta_{e,HPRB}$), of 0.2 (Mahmoodlu et al., 2015) and a diffusion coefficient, D_{HPRB}, equal to the diffusion coefficient in air were assumed. From Table 1 it can be observed that a higher reactivity, i.e. higher value of k'', does not necessarily imply a lower diffusive reaction length. For instance, the reaction length range found for 1,1-DCE is only slightly higher than the one found for PCE, although PCE is noticeably less reactive with permanganate (see k'' values in Table 1). Similar considerations can be made also comparing the reaction lengths obtained for 1,1-DCE with those of TCE. This result is due to the higher Henry's constant and diffusion coefficient of 1,1-DCE compared to those of PCE and TCE. It is worth noting that the estimated range of L_R reported in Table 1 is only indicative since, for a site-specific evaluation, L_R should be estimated based on the effective diffusion coefficient and oxidant solubility expected in the field.

Table 2 reports the overall reactions for the oxidation of common chlorinated solvents and the corresponding values of the stoichiometric mass ratios between potassium permanganate and the contaminant of concern (γ). As expected, the lower the degree of chlorination of the solvent, the higher the amount of potassium permanganate required for its complete oxidation.

3. Results

3.1. Comparison with experimental results

The results provided by the analytical model developed in this work were compared with the vapor attenuation of TCE observed by Mahmoodlu et al. (2015) in lab-scale column tests performed using a HPRB of potassium permanganate. Values for input parameters required to run the simulations, such as the physical characteristics and the thickness of the unsaturated soil, were taken from Mahmoodlu et al. (2015). For the estimation of the diffusion coefficient in soil, D_{soil}, a water

Table 1
Diffusive reaction lengths (L_R) estimated for different chlorinated solvents based on the second-order oxidation rate constants reported in the recent literature for permanganate. We assumed C_{ox} equal to the solubility of potassium permanganate at 20 °C (64 g/l), a relative water saturation of S^w of 0.2 and a diffusion coefficient, D_{HPRB}, equal to the value of the diffusion coefficient in air.

Compound	H[g] (−)	D_{HPRB}[g] (cm^2/s)	k'' ($M^{-1}\ s^{-1}$)	L_R (cm)
PCE	0.724	0.0505	0.0084–0.051[a]	5–12.4
TCE	0.403	0.0687	0.24–1.19[a,b,c,d]	0.9–2.0
cis-1,2-DCE	0.167	0.0884	0.69–1.78[a]	0.5–0.9
trans-1,2-DCE	0.167	0.0876	30–56.8[a]	0.1–0.13
1,1-DCE	1.07	0.0863	2.1–2.38[a]	1.17–1.25
VC	1.14	0.107	First-order (s^{-1}): 0.0137–0.0286[e]	7.8–11.3[f]

[a] Waldemer and Tratnyek (2006).
[b] Urynowicz (2007).
[c] Kao et al. (2008).
[d] Mahmoodlu et al. (2014b).
[e] Huang et al. (2001) have shown that the degradation of VC by permanganate is a two-consecutive-step process. The second step, being the rate-limiting step, is of first-order. The values reported in the table refer to the first-order constants obtained by these authors.
[f] The diffusive reaction lengths for VC were calculated with the first-order reaction constant (k') reported in the table using the following equation: $L_R = \sqrt{(D_{HPRB} \cdot H)/(k' \cdot \theta_{w,HPRB})}$.
[g] U.S.EPA (2015c).

saturation of S^w equal to 0.4 was considered representative of the average values of the soil water distribution reported by Mahmoodlu et al. (2015). The diffusive reaction length (L_R), which as shown in Eq. (6) depends on the second-order rate oxidation constant (k''), the water-filled porosity in the HPRB and the chemico-physical properties of the contaminants (in terms of H and D_{HPRB}), was determined by fitting the model to experimental results. As shown in Fig. 2, the simulations closely describe the experimental trends observed in the column oxidation tests. Furthermore, it is worth noting that the diffusive reaction lengths estimated for TCE by fitting the experimental results are within the range of L_R values reported in Table 1, demonstrating the applicability of the analytical approach proposed in this work. The slight different values of L_R observed for the two tests can be explained by differences in the actual diffusion coefficient of TCE through the 4 cm and the 8 cm thick barriers. In particular, the ratio of the TCE diffusive reaction lengths in the two cases can be estimated, assuming constant values of C_{ox}, k'', $\theta_{w,HPRB}$ and H, from Eq. (6) as:

$$\frac{L_{R(\text{test 1})}}{L_{R(\text{test 2})}} = \left(\frac{D_{HPRB(\text{test 1})}}{D_{HPRB(\text{test 2})}}\right)^{1/2} \tag{26}$$

Substituting the expression of D_{HPRB} reported in Eq. (2) and assuming the same D_a and $\theta_{e,HPRB}$ for test 1 and test 2, Eq. (26) can be written as:

$$\frac{L_{R(\text{test 1})}}{L_{R(\text{test 2})}} = \left(\frac{\theta_{a,HPRB(\text{test 1})}}{\theta_{a,HPRB(\text{test 2})}}\right)^{5/3} \tag{27}$$

Hence, the different L_R values estimated for the two tests can be ascribed to a different air-filled porosity of the reactive layers employed in the experiments. In particular, rearranging Eq. (27), the ratio of the air-filled porosity in the two tests can be estimated as:

$$\frac{\theta_{a,HPRB(\text{test 1})}}{\theta_{a,HPRB(\text{test 2})}} = \left(\frac{L_{R(\text{test 1})}}{L_{R(\text{test 2})}}\right)^{3/5} \tag{28}$$

Considering that the L_R ratio for the two tests is around 0.61 ($L_{R(\text{test 1})} = 1.1$ cm and $L_{R(\text{test 2})} = 1.8$ cm), from Eq. (28) an air-filled porosity ratio of 0.75 is expected. This means that, assuming an air-filled porosity of 0.28 (Mahmoodlu et al., 2015) for test 1, the air-filled porosity that could explain the different L_R value obtained for test 2 should be 0.21, which looks a reasonable value.

Finally, from Fig. 2 it can be also observed that nearly steady-state conditions were reached already after 20 h from the beginning of the tests, thus suggesting that transient conditions can be reasonably neglected for the design of HPRBs.

Table 2
Stoichiometric reaction of different chlorinated solvents with potassium permanganate.

Compound	Reaction with potassium permanganate	γ (g_{ox}/g_{VOC})
PCE	$4KMnO_4 + 3C_2Cl_4 + 4H_2O \rightarrow 4MnO_2 + 6CO_2 + 4K^+ + 8H^+ + 12Cl^-$	1.3
TCE	$2KMnO_4 + C_2HCl_3 \rightarrow 2MnO_2 + 2CO_2 + 2K^+ + H^+ + 3Cl^-$	2.4
cis-1,2-DCE *trans*-1,2-DCE 1,1-DCE	$8KMnO_4 + 3C_2H_2Cl_2 \rightarrow 8MnO_2 + 6CO_2 + 8K^+ + 2OH^- + 2H_2O + 6Cl^-$	4.3
VC	$10KMnO_4 + 3C_2H_3Cl \rightarrow 10MnO_2 + 6CO_2 + 10K^+ + 7OH^- + H_2O + 3Cl^-$	8.4

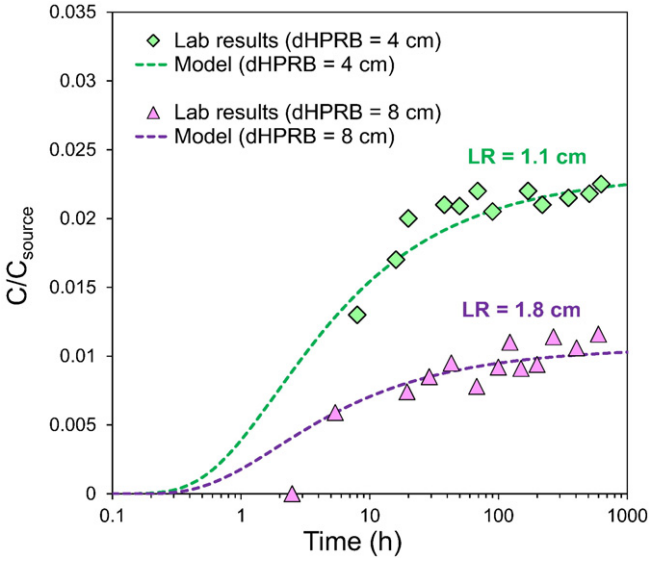

Fig. 2. Comparison of the TCE vapor attenuation simulated by the proposed model with the experimental results observed by Mahmoodlu et al. (2015) employing a potassium permanganate layer with a thickness of either 4 (test 1) or 8 cm (test 2). Here we assumed $\theta_{e,soil} = 0.35$, $h_{soil} = 7$ cm and an average relative water saturation in the soil of $S^w = 0.4$.

3.2. Estimation of minimum HPRB thickness required to attenuate vapors at acceptable levels

Fig. 3 shows, for different diffusive reaction lengths (L_R), the minimum HPRB thickness (d^*_{HPRB}) needed to attenuate vapors below risk-based soil-gas screening levels, estimated with Eq. (8) as a function of the required attenuation factor (C_{target}/C_{source}). Hence, based on the type of VOC and on the source concentration, Fig. 3 can help to design the reactive layer. For this purpose, the range of the diffusive reaction lengths expected for the different contaminants of concern are also reported as reference. As described in more detail in Section 2.2.4, the range of L_R for each contaminant shown in Fig. 3 was estimated based on the second-order rate oxidation constants available in the recent literature for $KMnO_4$ (see Table 1).

Let us consider the case of TCE. Based on Table 1, the upper bound of the reaction length (L_R) reported for TCE is equal to approximately 2 cm. Assuming a vapor source concentration of TCE equal to 1 g/m^3 and a soil-gas risk-based screening level of $1.59 \cdot 10^{-5}$ g/m^3 (U.S.EPA, 2015b), the required attenuation factor would be $1.59 \cdot 10^{-5}$. Using these values, from Fig. 3 the minimum HPRB thickness required to attenuate TCE vapors below acceptable levels would be around 20 cm. For PCE, assuming the same vapor source concentration and a risk-based soil vapor concentration of $3.5 \cdot 10^{-4}$ g/m^3 (U.S.EPA, 2015b), the attenuation factor would be $3.5 \cdot 10^{-4}$. Considering a reaction length for PCE equal to 2 cm, a minimum HPRB thickness around 120 cm would be required.

3.3. Estimation of the HPRB overdesign thickness

As mentioned in Section 2.2, when calculating the overall HPRB thickness, an overdesign term must be considered accounting for two processes, i.e. oxidation reactions and leaching, which simultaneously contribute to the depletion of a HPRB in field applications.

In order to assess the relative contribution of oxidation and leaching on the HPRB depletion, in this section we calculate the overdesign of the layer thickness needed to guarantee the barrier effectiveness for a set timeframe, relying on simulations carried out accounting separately for the permanganate consumption due to oxidation (Fig. 4) and leaching (Fig. 5).

The overdesign thickness needed to account for the oxidant consumption due to its reaction with upward diffusing vapors is reported in Fig. 4 for different diffusive reaction lengths (Eq. (18)). Based on the column tests performed by Mahmoodlu et al. (2015), here we considered a barrier constituted by a mixture of potassium permanganate and sand, hence estimating the HPRB density, ρ_{HPRB}, and the mass ratio of oxidant over the total mass in the reactive layer, η, applying Eqs. (15) and (16), respectively ($\eta = 0.5$; $\rho_{HPRB} = 1.74$ g/cm^3). As to the physical characteristics of the soil, a diffusion coefficient through the HPRB of 0.1 cm^2/s was assumed, which can be considered as an upper bound of the diffusion coefficient in air of the compounds of concern (see Table 1). From Fig. 4 it can be readily checked that, as expected, the higher the reaction length (i.e. lower reactivity) the longer the HPRB duration. For instance, assuming a total source concentration (γ C_{source}) equal to 1 g/m^3 and a reaction length of 5 cm (see Fig. 4c), an overdesign thickness of less than 10 cm is needed to ensure a HPRB duration of 10 years. Assuming a twice diffusive reaction length (see Fig. 4d), to ensure a HPRB duration of 10 years, a half of Δd_{HPRB} is needed (i.e. less than 5 cm). Obviously, in less severe contamination scenarios (e.g. assuming a total vapor source concentration lower than 1 g/m^3), the HPRB lifetime is expected to noticeably increase. For instance, it can be readily checked that, considering a γ C_{source} equal to 0.1 g/m^3, an increase in the HPRB thickness of 10 cm can ensure a mitigation system at high-level performance for at over 20 years even in the case of very reactive layers, i.e. in the case of relatively low diffusive reaction lengths (see e.g. Fig. 4a).

The contribution of oxidant dissolution and leaching on the HPRB depletion can be evaluated using Fig. 5, which shows the barrier overdesign thickness (Eq. (21)) needed to ensure a given HPRB lifetime as a function of the infiltration rate. To run these simulations we assumed again $\eta = 0.5$ and $\rho_{HPRB} = 1.74$ g/cm^3 (Mahmoodlu et al., 2015) and a potassium permanganate solubility of 64 g/l at 20 °C (Mahmoodlu et al., 2014a, b). Considering a sandy soil ($\beta = 0.0018$) and an average rainfall rate of 100 cm/year, i.e. an infiltration rate of 18 cm/year (Eq. (22)), from Fig. 5 it can be estimated that an overdesign thickness of 20 cm is needed to guarantee effective performance of the HPRB for a period of about 20 years.

By comparing Figs. 4 and 5, it can be also noted that, for high source concentrations, the HPRB lifetime is mostly affected by the oxidant consumption while for relatively low source concentrations (e.g. lower than 1 g/m^3) and high reaction lengths (e.g. higher than 5 cm), the HPRB depletion is mainly controlled by the dissolution and leaching of permanganate by infiltrating water. Namely, equating Eqs. (18) and (21), the infiltration rate, I_{ef}, above which the HPRB depletion will be controlled by permanganate leaching can be estimated as follows:

$$I_{ef} > \frac{1}{S_{ox}} \sum_{i=1}^{n} \gamma_i \cdot C_{HPRB,in,i} \cdot \frac{D_{HPRB,i}}{L_{R,i}} \tag{29}$$

From this equation it can be readily checked that for relatively low source concentrations (e.g. 1 g/m^3) and relatively high diffusive reaction lengths (e.g. 5 cm), infiltration rates higher than 10 cm/year are expected to control the HPRB depletion.

3.4. Possible geotechnical issues related to barrier depletion

Depending on the properties of the soil-permanganate mixture (e.g. soil grain size, relative amount of permanganate) the permanganate used may not just contribute to the reactivity but also to the structural properties of the HPRB. In such cases, the HPRB depletion due to oxidation can lead to a progressive compaction of the reactive layer due to the overburden pressure resulting from the soil overlying the reactive barrier. In the case of a HPRB containing a permanganate mixture, it should be considered that $KMnO_4$ generates solid insoluble manganese dioxides (MnO_2) in the reaction with the target compounds (MacKinnon and Thomson, 2002; Xu and Thomson, 2009; Cha and Borden, 2012). For in situ chemical oxidation in groundwater, the MnO_2 production represents an undesirable side-effect to be managed since MnO_2

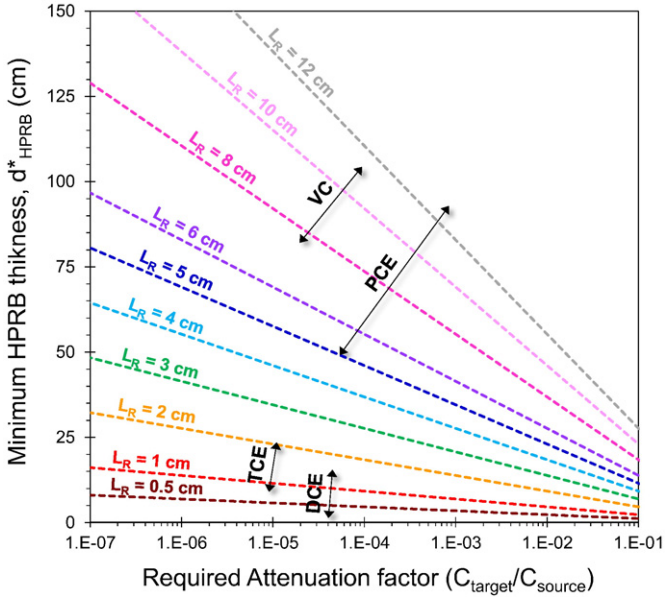

Fig. 3. Minimum HPRB thickness, d^*_{HPRB}, estimated as a function of the required attenuation factor, C_{target}/C_{source}, based on the diffusive reaction length, L_R.

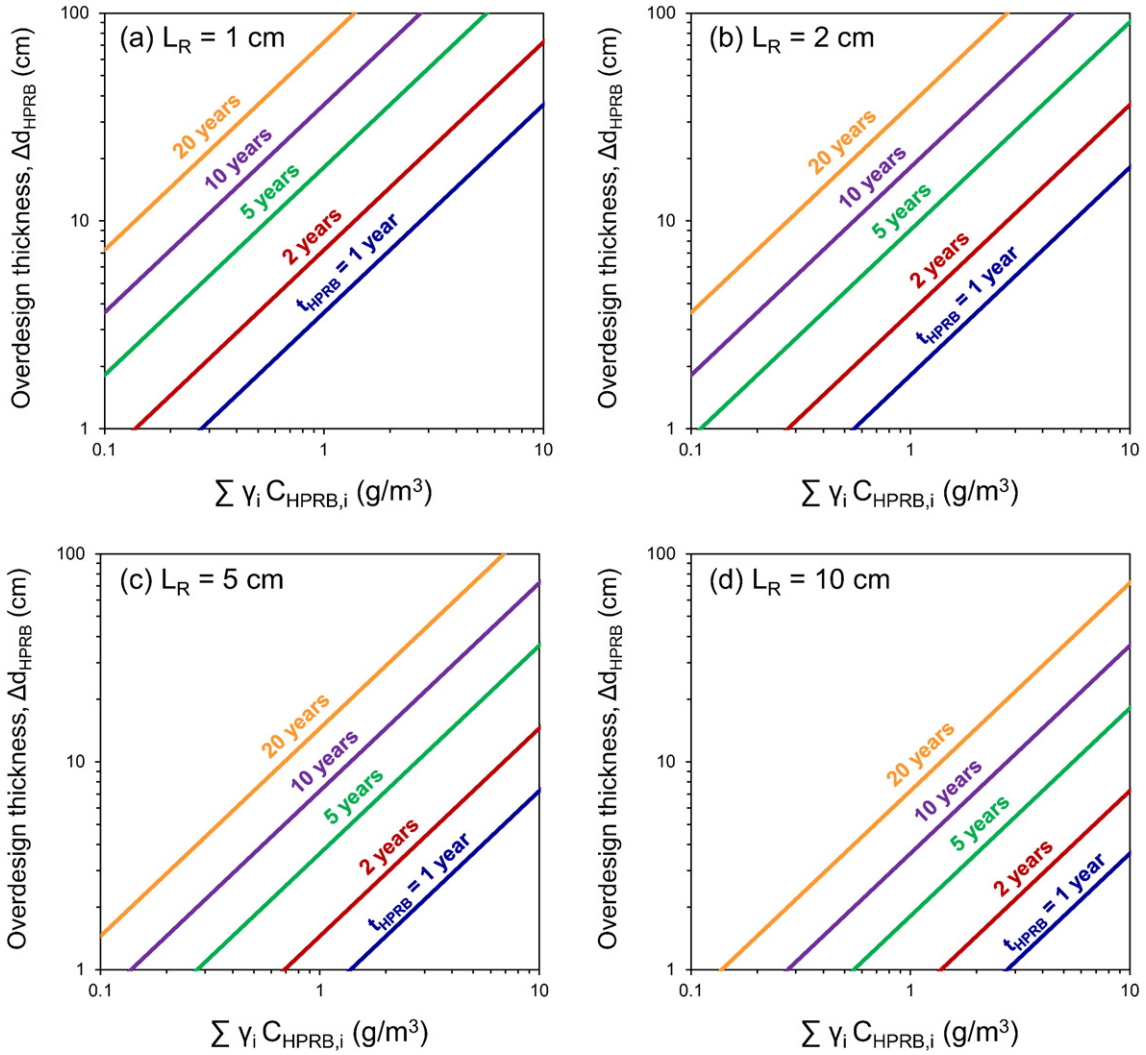

Fig. 4. Estimated HPRB overdesign thickness (Δd_{HPRB}) due to oxidation required to attenuate VOCs at acceptable risk-based levels for different HPRB lifetimes and contaminants type and concentration, assuming: (a) $L_R = 1$ cm, (b) $L_R = 2$ cm, (c) $L_R = 5$ cm and (d) $L_R = 10$ cm. Here we assumed $\eta = 0.5$, $D_{HPRB} = 0.1$ cm^2/s and $\rho_{HPRB} = 1.74$ g/cm^3.

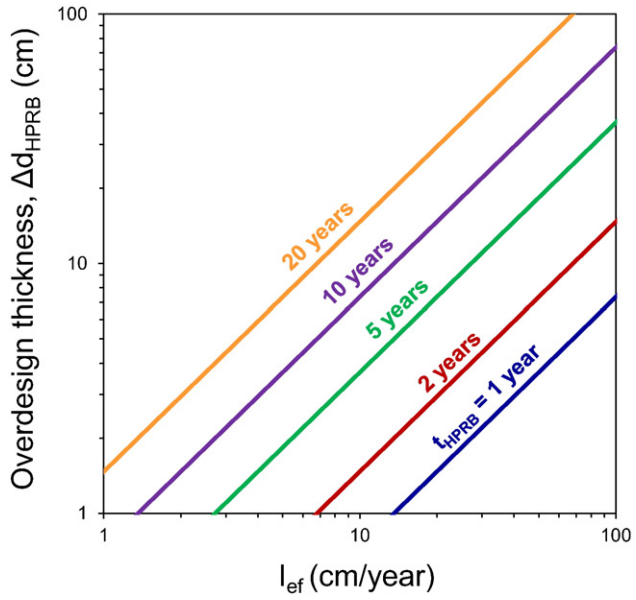

Fig. 5. Estimated HPRB overdesign thickness (Δd_{HPRB}) due to permanganate leaching required to attenuate VOCs at acceptable risk-based levels for different HPRB lifetimes assuming. Here we assumed $S_{ox} = 64$ g/l, $\eta = 0.5$, and $\rho_{HPRB} = 1.74$ g/cm^3.

particles can deposit in the subsurface and impact the soil permeability around the injection well (Crimi et al., 2009; Baciocchi et al., 2014). By contrast, for a HPRB application the production of solid MnO_2 represents a positive side effect since it moderates the geotechnical issues related to the progressive compaction of the reactive layer due to oxidant consumption. Namely, at a generic time t, the volume of the barrier occupied by the oxidant and its by-product (MnO_2) can be estimated as follows:

$$V_{oxidant}(t) = \frac{M_{KMnO4}(t)}{\rho_{KMnO4}} + \frac{M_{MnO2}(t)}{\rho_{MnO2}} \tag{30}$$

where $M_{KMnO4}(t)$ is the mass of potassium permanganate in the barrier, $M_{MnO2}(t)$ the mass of manganese dioxides generated from the reaction of $KMnO_4$ with the target compounds and ρ_{KMnO4} and ρ_{MnO2} the particle density of potassium permanganate and manganese dioxides, respectively. The stoichiometric molar ratio of MnO_2 produced per $KMnO_4$ reacted with a generic chlorinated solvent is 1:1 (see Table 2) and hence considering the molecular weight of $KMnO_4$ and MnO_2 (158.034 g/mol and 86.9368 g/mol, respectively), 0.55 g of MnO_2 are produced for 1 g of reacted $KMnO_4$ (i.e. $\gamma_{MnO2} = 0.55$ g_{MnO2}/g_{KMnO4}). Hence Eq. (30) can be rewritten as:

$$V_{oxidant}(t) = \frac{M_{KMnO4}(t)}{\rho_{KMnO4}} + \frac{[M_{KMnO4}(t=0) - M_{KMnO4}(t)] \cdot \gamma_{MnO2}}{\rho_{MnO2}} \tag{31}$$

where $M_{KMnO4}(t=0)$ is the initial mass of $KMnO_4$ present in the reactive barrier.

Normalizing the volume at time t for the initial volume occupied by potassium permanganate, the volume reduction can be estimated as follows:

$$\frac{V_{oxidant}(t)}{V_{oxidant}(t=0)} = \frac{\frac{M_{KMnO4}(t)}{\rho_{KMnO4}} + \frac{[M_{KMnO4}(t=0) - M_{KMnO4}(t)] \cdot \gamma_{MnO2}}{\rho_{MnO2}}}{\frac{M_{KMnO4}(t=0)}{\rho_{KMnO4}}} \quad (32)$$

At end of HPRB lifetime (i.e. $M_{KMnO4}(t)=0$), Eq. (32) reduces to:

$$\frac{V_{oxidant}(t=t_{HPRB})}{V_{oxidant}(t=0)} = \frac{\gamma_{MnO2} \cdot \rho_{KMnO4}}{\rho_{MnO2}} \approx 0.3 \quad (33)$$

Hence considering the particle density of $KMnO_4$ and MnO_2 (2.703 g/cm^3 and 5.026 g/cm^3, respectively) from Eq. (33) it can be estimated that approximately 30% of the initial volume occupied by potassium permanganate will be replaced for by MnO_2 at end of HPRB lifetime, i.e. a volume reduction of 70% is expected.

Finally, considering that the HPRB barrier is usually composed of a mixture of potassium permanganate and sand, the initial volume of the barrier occupied by the oxidant compared to the total HPRB volume can be estimated as follows:

$$\frac{V_{oxidant}(t=0)}{V_{HPRB}(t=0)} = \frac{\frac{M_{oxidant}}{\rho_{oxidant}}}{\left[\frac{M_{sand}}{\rho_{sand}} + \frac{M_{oxidant}}{\rho_{oxidant}}\right]\left(\frac{1}{1-\theta_{e,HPRB}}\right)} \quad (34)$$

Considering that the particle density of permanganate is similar to that of sand (i.e. $\rho_{KMnO4} = 2.703$ g/cm^3 and $\rho_{sand} = 2.65$ g/cm^3), Eq. (34) can be approximated to:

$$\frac{V_{oxidant}(t=0)}{V_{HPRB}(t=0)} \approx \eta(1-\theta_{e,HPRB}) \quad (35)$$

At the end of HPRB lifetime the reduction of the barrier volume will be hence equal to:

$$\frac{V_{HPRB}(t=t_{HPRB})}{V_{HPRB}(t=0)} \approx 1-\left(1-\frac{V_{oxidant}(t=t_{HPRB})}{V_{oxidant}(t=0)}\right)\eta(1-\theta_{e,HPRB}) \quad (36)$$

Assuming $\eta = 0.5$ and $\theta_{e,HPRB} = 0.35$ (Mahmoodlu et al., 2015), the final volume of HPRB will be 77% of the initial value (i.e. a volume reduction of 23% will be attained). Hence, for a 100 cm thick HPRB, a maximum compaction of around 23 cm is foreseen at the end of barrier lifetime (that can be in the order of several years). This means that a subsidence of a few centimeters per year can be expected. This might not be an issue for open ground applications while it should be surely addressed in the case of installation of HPRBs below buildings, depending on the type of building foundations (e.g. shallow or deep foundations). For instance, in the case of shallow building foundations (e.g. slab-on-grade foundations) a supporting frame containing the reactive layer can be adopted to avoid any possible geotechnical issue.

3.5. Influence of site-specific parameters on the HPRB performance

Although field tests are required to assess actual performance of HPRBs and the importance of the discussed parameters, in this section, we briefly evaluate how key site-specific parameters may be of influence using the theoretical considerations presented in this study.

3.5.1. Water content in the reactive barrier

Modifications of the water content in the reactive barrier ($\theta_{w,HPRB}$) can affect the HPRB performance in terms of oxidation rate (see Eq. (1)) and, indirectly, of diffusion of VOCs through the HPRB (see Eq. (2)). Specifically, the higher the water content, the higher the oxidation rate and the slower the VOCs diffusion through the barrier. As a consequence, also the diffusive reaction length, given by Eq. (6), is affected, both directly and indirectly, by the water content in the reactive barrier. This is shown in Fig. 6a where the diffusive reaction length (L_R), normalized to a reference L_R calculated for $S^w = 20\%$, is reported for a range of relative water saturation ($S^w = \theta_{w,HPRB} / \theta_{e,HPRB}$) values, while keeping constant the other parameters that affect the diffusive reaction length (i.e. k'', H, D_{HPRB}, C_{ox} in Eq. (6)). Looking at Fig. 6a, in the case of a reduction of S^w from 20% to 10%, the reaction length is expected to increase of a factor 1.7. Hence, assuming a reaction length of $L_R = 2$ cm (e.g. for TCE) and a thickness of the HPRB of 20 cm, from Eq. (7) it can be estimated that the vapor attenuation through the HPRB would change from a value of around $4.5 \cdot 10^{-5}$ ($L_R = 2$ cm) to a value of $2.8 \cdot 10^{-3}$ ($L_R = 3.4$ cm), i.e. a variation of almost two orders of magnitude. By contrast, an increase of the water content would enhance the HPRB performance. For instance, in the case of an increase of S^w from 20% to 40%, the reaction length is expected to decrease of a factor 0.5. This reduction of L_R would correspond, for the example reported above (i.e. a thickness of

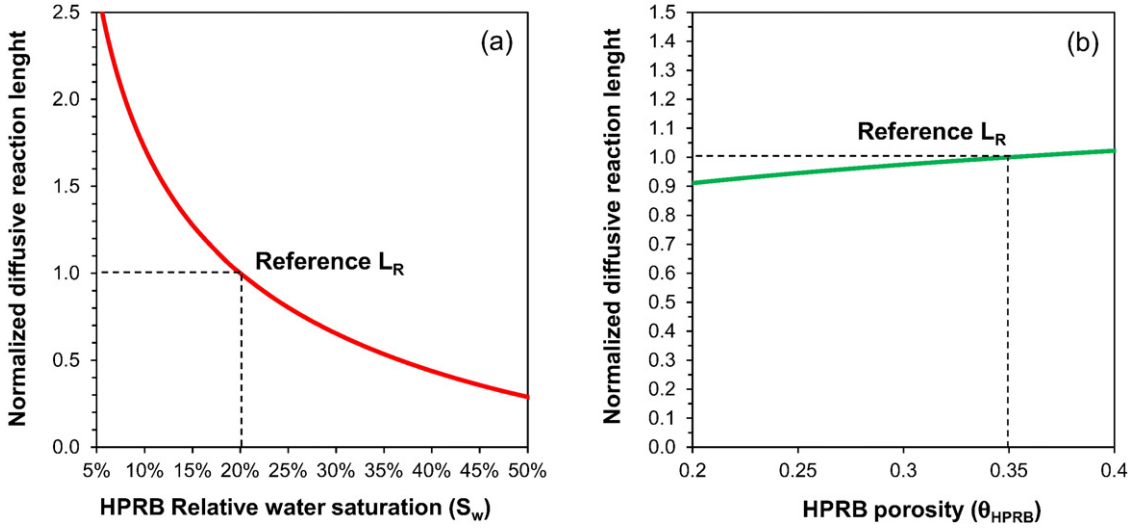

Fig. 6. Normalized diffusive reaction length as a function of (a) the HPRB relative water saturation ($S^w = \theta_{w,HPRB} / \theta_{e,HPRB}$) and (b) the HPRB porosity ($\theta_{e,HPRB}$). The diffusive reaction lengths are normalized to the reference diffusive reaction length calculated for a relative water saturation $S^w = 0.2$ and a HPRB porosity $\theta_{e,HPRB} = 0.35$.

the HPRB of 20 cm), to an attenuation factor of $2.1 \cdot 10^{-9}$ ($L_R = 1$ cm). Based on these results, to ensure an adequate performance of the reactive barrier, it is recommended, especially during the warmer months, to carefully monitor and control the moisture content in the reactive barrier. Conversely, during wet periods the moisture content might be not an issue as an enhancement of the HPRB performance is expected.

3.5.2. Porosity of the reactive barrier

As discussed above, the HPRB depletion due to oxidation might lead to a progressive reduction of the barrier porosity as a result of compaction by the overlying soil. To evaluate how this compaction can influence the HPRB performance in terms of vapors attenuation, Fig. 6b reports the diffusive reaction length (L_R), normalized to a reference L_R calculated for $\theta_{e,HPRB} = 0.35$, for a range of HPRB effective porosity ($\theta_{e,HPRB}$) values. For this estimation, a constant relative water saturation, S^w, equal to 20% was assumed. From this figure it can be observed that the reduction of the HPRB porosity only slightly affects the diffusive reaction length. For instance, assuming an initial $\theta_{e,HPRB} = 0.35$ and considering a reduction of the porosity of 23% (i.e. $\theta_{e,HPRB} = 0.27$), the diffusive reaction length is expected to decrease of 5% (i.e. a normalized diffusive reaction length equal to 0.95). This means that the progressive compaction of the HPRB would slightly enhance the HPRB performance over time. Indeed, assuming a constant relative water saturation in the barrier, a decrease of the HPRB porosity would lead to a corresponding decrease of the air-filled porosity and hence of the diffusion coefficient through the barrier (see Eq. (2)). Overall this would lead to a lower diffusive reaction length (see Eq. (6)) and consequently to an enhanced attenuation of vapors through the barrier. Thus summarizing, based on our calculations, in the case of contaminants transport through the HPRB governed by diffusion, a porosity reduction of 23% would only slightly affect the performance of the mitigation system. However, it should be considered that for applications in coarse soils, a reduction of the air-filled porosity in the HPRB due to its progressive compaction could lead to the formation of a layer characterized by a lower permeability to vapors compared to the native soil. This might lead to an accumulation of vapors at the soil to HPRB interface that could induce the formation of lateral concentration gradients, thus enhancing the lateral diffusion of vapors beyond the perimeter of the barrier. Due to the 1-D nature of the model developed in this work, this side-effect cannot be quantified. However, in order to limit the possibility of lateral by-pass of vapors, a barrier wider than the source footprint should be foreseen.

It is worth noting that the above considerations are valid for a constant relative water saturation during compaction. However, if the progressive compaction would lead to a change of the moisture content, the reactivity of HPRB can significantly change. In this case readers should refer to the results shown in Fig. 6a and discussed in the previous section.

3.5.3. Temperature

As for the effects of temperature on HPRB performance, the higher the temperature, the higher the oxidation rate constant k'', as described by the Arrhenius equation:

$$k'' = A \cdot \exp\left(-\frac{E_a}{RT}\right) \tag{37}$$

where A is the pre-exponential factor, E_a the activation energy (kcal mol^{-1}), R the universal gas constant and T the temperature (K).

Huang et al. (2001) estimated an activation energy for the reactions between $KMnO_4$ and chlorinated ethenes of 9.3 kcal mol^{-1} (PCE), 8.9 kcal mol^{-1} (TCE), 8.8 kcal mol^{-1} (*cis*-1,2-DCE), 6.9 kcal mol^{-1} (1,1-DCE) and 5.8 kcal mol^{-1} (*trans*-1,2-DCE). For VC, the same authors have shown that its degradation by permanganate is a two-consecutive-step process, with the second being the rate-limiting step, with an activation energy of 7.9 kcal mol^{-1}.

From Eq. (37), it can be estimated that, independently from the pre-exponential factor, A, a 10 °C decrease of the temperature will lead to a decrease of the oxidation rate by a factor of 1.8 for PCE and a factor of 1.4 for *trans*-1,2-DCE.

On the other hand, a temperature decrease would lead to a lower solubility of the oxidant. For $KMnO_4$, the solubility would decrease from 64 g/l at 20 °C to 44 g/l at 10 °C (Water Security Agency, 2016), i.e. a reduction factor of solubility of 1.45 would be achieved.

Overall, a 10 °C decrease would lead to an increase of the diffusive reaction length of 1.6 for PCE to 1.4 for *trans*-1,2-DCE (Eq. (6)). For instance, considering an initial reaction length of $L_R = 8$ cm (e.g. for PCE) and a thickness of the HPRB of 80 cm, from Eq. (7) it can be estimated that the vapor attenuation through the HPRB would change from around $4.5 \cdot 10^{-5}$ (e.g. at 20 °C) to around $1.9 \cdot 10^{-3}$ for a temperature decrease in the barrier of 10 °C (i.e. assuming an increase of the diffusive reaction length to $L_R = 12.7$). This means that during the cold season and especially during dry periods, the efficiency of the reactive barrier could be sensibly reduced. Conversely, during rainy periods, the effect of the temperature on the oxidation rate could be mitigated by the higher water content in the HPRB, that as discussed in the previous section may enhance the HPRB performance.

3.5.4. pH

The reaction of chlorinated solvents with MnO_4^- can lead to the formation of acids (e.g. carboxylic acids) that can cause a progressive drop of pH to acidic values (Yan and Schwartz, 1999). Previous studies showed that permanganate oxidation with chlorinated solvents is independent from pH in the range of 4 to 8 (Yan and Schwartz, 1999; Kao et al., 2008). At lower pH values, Mahmoodlu et al. (2015) observed a reduction in HPRB reactivity in their lab-scale tests.

The effects of pH on the oxidation rate constant can be described with the following equation (Mahmoodlu et al., 2014a):

$$k''(pH<4) = k'' \cdot (pH-a)^b \tag{38}$$

in which k'' denotes the reaction rate constant in water whereas a and b are empirical parameters. For TCE, Mahmoodlu et al. (2014a) have estimated a value of $a = 1.25$ and $b = 2$. This means that, in the case of a drop of pH from 4 to 2, independently from the value of k'', a decrease of the oxidation rate of a factor of 13.4 is expected. This reduction of reactivity would correspond to an increase of the diffusive reaction length of a factor 3.6 (see Eq. (6)).

In field applications, it is reasonable to expect that the effect of pH on the oxidation rate would be limited since the infiltrating water might periodically neutralize the drop of pH to acidic value. This conjecture is partially supported by the results obtained by Mahmoodlu et al. (2015) who, in some experiments, did not observe any effect of pH, presumably due to the diffusion of protons or hydroxide ions away from the HPRB, especially downwards to the higher water saturation area.

3.5.5. Attenuation of vapors in the soil below the barrier

The results shown in this paper were obtained assuming a negligible attenuation of vapors through the soil column between the source and the HPRB. Although this assumption ensures a conservative design of the HPRB thickness, in some cases cannot reflect the real behavior expected in the field.

At steady-state, the flux of vapors through the soil can be estimated as follows:

$$J_{soil} = D_{soil} \cdot \frac{C_{source} - C_{HPRB,in}}{h_{soil}} \tag{39}$$

where h_{soil} is the thickness of the soil below the reactive barrier.

By equating the fluxes (Eqs. 39 and (10)) at the soil to HPRB interface, the attenuation factor of vapors in the soil (α_{soil}) can be estimated

as:

$$\alpha_{soil} = \frac{C_{HPRB,in}}{C_{source}} = \frac{1}{1 + \frac{D_{HPRB} \cdot h_{soil}}{D_{soil} \cdot L_R}} \quad (40)$$

Substituting D_{soil} and D_{HPRB} with the Millington and Quirk (1961) equation expression described in Eq. (2), Eq. (40) becomes:

$$\alpha_{soil} = \frac{1}{1 + \frac{\theta_{a,HPRB}^{10/3} \cdot \theta_{e,soil}^{2} \cdot h_{soil}}{\theta_{a,soil}^{10/3} \cdot \theta_{e,HPRB}^{2} \cdot L_R}} \approx \frac{1}{1 + \frac{\theta_{a,HPRB}^{10/3} \cdot h_{soil}}{\theta_{a,soil}^{10/3} \cdot L_R}} \quad (41)$$

Assuming a similar porosity in the soil and in the reactive barrier, the attenuation factor in the soil can be estimated as reported in the right hand of Eq. (41).

Fig. 7 shows the attenuation factor in the soil ($\alpha_{soil} = C_{HPRB,in} / C_{source}$) calculated with Eq. (41) as a function of the ratio of the soil thickness to the diffusive reaction length (h_{soil}/L_R) for different air-filled porosity in the HPRB ($\theta_{a,HPRB}$) and in the soil ($\theta_{a,soil}$). From this figure it can be observed that, depending on the differences between the air-filled porosity in the HPRB and the air-filled porosity in the soil (and hence indirectly of the water content), the extent of the attenuation of vapors through the soil can significantly change. For instance, in the case of a barrier installed near the source (e.g. $h_{soil}/L_R = 1$), the attenuation factor in the soil may change up to 1 order of magnitude, i.e. from a value of 1 for an air-filled porosity in the soil higher than the one in the HPRB ($\theta_{a,HPRB} / \theta_{a,soil} = 0.5$) to a value of 0.1 for $\theta_{a,HPRB} / \theta_{a,soil} = 2$. In the case of a greater soil thickness or a lower diffusive reaction length, i.e. for higher values of the ratio h_{soil}/L_R, a low air filled porosity in the soil ($\theta_{a,HPRB} / \theta_{a,soil} = 2$) can lead to an attenuation of vapor concentrations below the barrier up to 3 orders of magnitude.

3.6. Demonstrative application

In this section we briefly discuss the design of a permanganate HPRB for the mitigation of the volatilization pathway at a sample site, where a dry cleaner and laundry facility was located, contaminated by chlorinated solvents due to discharge of dry cleaning waste to the storm sewer. The soil of the site is a fine-grained sand, whereas the groundwater table is between 5 and 6 m below ground. Environmental investigations on groundwater samples indicated a contamination by chlorinated solvents for an area of about 200 m^2, revealing maximum concentrations of PCE and TCE equal to 4 and 35 mg/l, respectively. For the design of the HPRB with potassium permanganate, the first step is to estimate the expected soil-gas concentration. Based on the maximum groundwater concentrations, the soil-gas concentrations, C_{source}, are expected to be around 0.11 g/m^3 for PCE and 0.55 g/m^3 for TCE. Thus, the minimum HPRB thickness required to attenuate vapors at acceptable levels can be estimated with Eq. (8), assuming the soil-gas risk-based screening levels and the reaction lengths reported in Table 3. The resulting minimum HPRB thicknesses would be in the order of 72 cm for PCE and 21 cm for TCE. Therefore, a HPRB with a

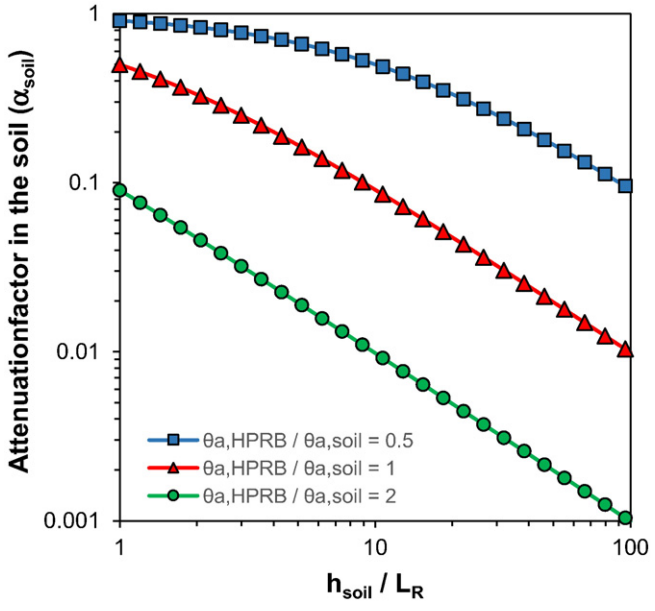

Fig. 7. Attenuation factor in the soil ($\alpha_{soil} = C_{HPRB,in} / C_{source}$) calculated as a function of the ratio of the soil thickness to the diffusive reaction length (h_{soil}/L_R) for different air-filled porosity in the HPRB ($\theta_{a,HPRB}$) and in the soil ($\theta_{a,soil}$).

Table 3
HPRB design parameters for the sample site considered in this work.

Parameter	Unit	Value		Notes
Contaminant properties				
		PCE	TCE	
$C_{gw,max}$	mg/l	4	35	Site-specific
H	–	0.724	0.403	U.S.EPA (2015c)
D_{HPRB}	cm^2/s	0.0505	0.0687	U.S.EPA (2015c)
C_{source}	g/m^3	0.11	0.55	Estimated as $C_{source} = C_{gw} \cdot H \cdot \alpha_{cap}$
C_{target}	g/m^3	$3.5 \cdot 10^{-4}$	$1.59 \cdot 10^{-5}$	U.S.EPA (2015b)
L_R	cm	12.4	2	Upper bound of values reported in Table 1
γ	$g'_{ox}g_{VOC}$	1.3	2.4	Estimated based on stoichiometric equation (see Table 2)
$J_{HPRB,layer}$	$g/m^2/d$	0.4	16	Estimated with Eq. (10)
Site characteristics				
Texture		Loamy sand		Site-specific
L	cm	550		Site-specific
$\theta_{e,soil}$	–	0.353		ISPRA (2008)
$\theta_{a,soil}$	–	0.25		ISPRA (2008)
$\theta_{a,cap}$	–	0.035		ISPRA (2008)
h_{cap}	cm	18.8		ISPRA (2008)
β	–	0.0018		Connor et al. (1997)
I_{ef}	cm/years	13		Estimated with Eq. (22) assuming $P = 85$ cm/years
α_{cap}	–	0.04		Estimated as reported by Verginelli and Baciocchi (2014)
HPRB design				
Barrier mixture		$KMnO_4$ + sand		Mahmoodlu et al. (2015)
S_{ox}	g/l	64		Mahmoodlu et al. (2014a, b)
θ_{HPRB}	–	0.35		Mahmoodlu et al. (2015)
ρ_{HPRB}	g/cm^3	1.74		Estimated with Eq. (16)
η	–	0.5		Estimated with Eq. (17)
A_{HPRB}	m^2	200		Site-specific
$t_{HPRB,desired}$	years	10		–
d^*_{HPRB}	cm	72		Maximum of the values estimated with Eq. (8) for PCE (72 TCE (21 cm)
Δd_{HPRB}	cm	26		Estimated with Eq. (24)
d_{HPRB}	cm	98		Estimated with Eq. (25)
M_{KMnO4}	tons	170		Estimated as $\eta \cdot \rho_{HPRB} \cdot d_{HPRB} \cdot A_{HPRB}$
M_{sand}	tons	170		Estimated as $(1 - \eta) \cdot \rho_{HPRB} \cdot d_{HPRB} \cdot A_{HPRB}$
$H_{excavation}$	cm	200		–
$H_{backfill}$	cm	102		Estimated as $H_{excavation} - d_{HPRB}$
$V_{excavation}$	m^3	400		Estimated as $H_{excavation} \cdot A_{HPRB}$
$V_{backfill}$	m^3	204		Estimated as $H_{backfill} \cdot A_{HPRB}$
V_{HPRB}	m^3	196		Estimated as $d_{HPRB} \cdot A_{HPRB}$
$V_{disposal}$	m^3	400		Equal to $V_{excavation}$

Table 4
Estimation of the HPRB capital costs for the sample site considered in this work.

Costs category	Unit cost (€/ton)	Quantity	Total costs (€)	Notes
$KMnO_4$	3,000	170 tons	510,000	Unit cost from ITRC (2001). Total costs were estimated based on the data reported in Table 3.
Excavation	–	400 m^3	8,431	Estimated as $7.43 \cdot V_{excavation} + 5{,}459$ (modified from U.S.EPA, 2004 for units conversion)
Backfill (HPRB)	–	196 m^3	3,444	Estimated as $17.57 \cdot V_{HPRB}$ (modified from U.S.EPA, 2004 for units conversion). The volume of the HPRB, V_{HPRB}, was estimated based on the data reported in Table 3.
Backfill (sand)	–	204 m^3	3,584	Estimated as $17.57 \cdot V_{backfill}$ (modified from U.S.EPA, 2004 for units conversion)
Disposal	139	680 tons	94,520	Unit cost refers to the disposal of hazardous waste without stabilization (U.S.EPA, 2001). Total costs were estimated based on the data reported in Table 3, assuming a soil bulk density equal to 1.7 ton/m^3.
Total			619,979	–

minimum thickness (d^*_{HPRB}) of 72 cm should be foreseen in order to achieve vapors attenuation to acceptable levels. Next, assuming 10 years as the desired timeframe of the mitigation system, the overdesign thickness of the barrier, accounting for depletion due to leaching and oxidation should be $\Delta d_{HPRB} = 26$ cm.

Thus a HPRB thickness of 98 cm ($d^*_{HPRB} + \Delta d_{HPRB}$) would ensure the treatment of PCE and TCE vapors at acceptable risk-based levels for at least 10 years. According to the composition, thickness and horizontal surface area of the designed barrier, the total amount of potassium permanganate and sand for the treatment of the contaminated area (approximately 200 m^2) would be around 170 tons each.

Based on the site characteristics and the HPRB design parameters, the bottom of the barrier was assumed to be installed at 2 m below ground, thus implying the excavation of about 400 m^3 of soil. The resulting excavated material was assumed to be transported in landfill for final disposal while a sandy soil obtained from an off-site source was supposed to be used as filling material in the remaining volume above the HPRB, i.e. about 200 m^3. Contamination characteristics, site properties and HPRB design parameters are summarized in Table 3.

Considering this specific configuration scenario, the estimated costs of the proposed mitigation system are reported in Table 4. As for the raw materials composing the barrier, the costs of the potassium permanganate were accounted only, as the contribution of sand to total costs was considered negligible. Costs related to the delivery, spreading and compaction of sand and $KMnO_4$ were taken into account by using the equation suggested by U.S.EPA (2004) for backfilling applications. According to our evaluation, the capital costs of the HPRB system for the presented case study would be in the order of 620,000 €, with a major contribution of the purchase price of the oxidant.

From Eq. (10) the total flux of PCE and TCE entering the barrier would be equal to 0.4 g/m^2/d and 16 g/m^2/d, respectively (see Table 3). Considering a complete oxidation of vapors within the HPRB, the total mass of VOC treated in the contaminated area of 200 m^2 after 10 years is equal up to 12.1 tons (0.3 tons of PCE and 11.8 tons of TCE). This means that the capital costs of this mitigation system would be likely in the order of 51 € per kg of VOC treated. It should be pointed out that the treatment of the same amount of contaminant (around 27,000 lb) using soil vapor extraction (SVE) systems would cost around 58 € per kg of VOC removed (30 $/lb), based on the data reported by U.S.EPA (2001). On the other hand, the operating and maintenance (O&M) costs of HPRB systems are likely lower compared to SVE systems. Indeed, the O&M costs of passive systems are actually negligible compared to those of SVE associated to the electricity, maintenance and monitoring of the extraction and treatment system. This hence suggests that HPRB systems may be feasible also from an economical point of view, particularly in the case of open ground applications or in the case of deep building foundations, where a compaction of the barrier of few centimeters in 10 year is likely to be not a geotechnical issue. However, in the case of an application below buildings with shallow foundations (e.g. slab-on-grade foundations), the costs would sensibly enhance as geotechnical mitigation strategies should be necessarily foreseen to maintain the infrastructure.

4. Conclusions

It is concluded that the proposed analytical model is able to closely replicate experimental results, and hence it can represent a valuable tool for the design of horizontal permeable reactive barriers (HPRBs). Simulation results confirmed that HPRBs of potassium permanganate is an effective mitigation system for chlorinated solvent vapors diffusing from contaminated soils and groundwater. Simulation outcomes highlighted that HPRBs of potassium permanganate with a thickness of less than 1 m are already able to attenuate chlorinated solvent vapors of orders of magnitude for several years. Indeed, the demonstrative application to a sample site showed that in the case of groundwater contamination by PCE and TCE of 4 mg/l and 35 mg/l, a barrier with a thickness of 1 m can ensure vapors attenuation at acceptable risk-based levels for at least 10 years. Furthermore, these results suggest that HPRB can be feasible also from an economical point of view, as the estimated capital costs are somewhat lower than the ones of other remediation options, such as soil vapor extraction systems. Overall, based on the experimental and theoretical evaluation thus far, future researches are warranted to verify the cost-effectiveness of HPRBs for vapor mitigation control under various conditions of application. To this end, pilot-scale field tests can be foreseen to evaluate the long-term performance of the mitigation system in terms of progressive compaction of the barrier, effect of possible clogging at the soil to barrier interface and additional costs for geotechnical mitigations strategies needed to maintain the infrastructure in the case of an application of the barrier below shallow building foundations.

Nomenclature

a	empirical parameter for the estimation of the effect of pH on the oxidation rate	–
A	pre-exponential factor in the Arrhenius equation	–
A_{HPRB}	horizontal surface area of the HPRB	m^2
b	empirical parameter for the estimation of the effect of pH on the oxidation rate	–
$C_{gw,max}$	groundwater maximum concentration	g/l
$C_{HPRB,in}$	vapor concentration of the compound entering the HPRB	g/m^3
C_{ox}	concentration of oxidant in the water phase	g/l
C_{source}	vapor concentration of the compound at the source	g/m^3
C_{target}	acceptable risk-based soil-gas concentration	g/m^3
C_v	concentration of contaminants in the soil-gas phase	g/m^3
D_a	diffusion coefficient of contaminants in air	m^2/h
d_{HPRB}	HPRB thickness	m
d^*_{HPRB}	minimum HPRB thickness to attenuate VOCs at acceptable levels	m
D_{HPRB}	effective porous medium diffusion coefficient through the HPRB	m^2/h
D_{soil}	effective porous medium diffusion coefficient through the soil	m^2/h
E_a	activation energy	kcal mol^{-1}
H	dimensionless Henry's law constant	–
h_{cap}	thickness of the capillary fringe	m
h_{soil}	vertical source to HPRB distance	m
$H_{excavation}$	depth of excavation	m
$H_{backfill}$	depth of sand backfilling	m

(*continued*)

I_{ef}	infiltration rate	cm/years
$J_{HPRB,layer}$	flux of vapors through the HPRB	g/m^2/d
k'	first-order oxidation rate constant	s^{-1}
k''	second-order oxidation rate constant	M^{-1} s^{-1}
L	groundwater depth	m
L_R	diffusive reaction length	m
$M_{oxidant}$	mass of oxidant in the HPRB	g
M_{sand}	mass of sand in the HPRB	g
M_{KMnO4}	mass of potassium permanganate in the HPRB	g
M_{MnO2}	mass of manganese dioxides in the HPRB	g
P	rainfall rate	cm/years
R	universal gas constant	J/mol K
S_{ox}	oxidant solubility	g/l
S^w	relative water saturation in the HPRB	–
$t_{HPRB,leach}$	lifetime of the HPRB due to leaching	years
$t_{HPRB,ox}$	lifetime of the HPRB due to oxidation	years
$t_{HPRB,desired}$	fixed time-framework for HPRB functioning	years
T	temperature	K
$V_{excavation}$	volume of excavated soil	m^3
$V_{backfill}$	volume of backfilling sand	m^3
$V_{disposal}$	volume of landfilled soil	m^3
V_{HPRB}	total HPRB volume	m^3
$V_{oxidant}$	volume of HPRB occupied by the oxidant	m^3
α_{cap}	attenuation factor in the capillary fringe	–
β	empirical factor for the estimation of the infiltration rate	–
γ	stoichiometric mass coefficient between the oxidant and the contaminant of concern	g_{ox}/g_{VOC}
γ_{MnO2}	stoichiometric mass coefficient between manganese dioxides and potassium permanganate	g_{KMnO4}/g_{MnO2}
Δd_{HPRB}	increase of the HPRB thickness needed to ensure a high-level performance	m
η	ratio of oxidant mass over the total mass in the HPRB	–
$\theta_{a,cap}$	air-filled porosity of the capillary fringe	–
$\theta_{a,HPRB}$	air-filled porosity of the HPRB	–
$\theta_{a,soil}$	air-filled porosity of the soil	–
$\theta_{e,HPRB}$	effective porosity of the HPRB	–
$\theta_{e,soil}$	effective soil porosity	–
$\theta_{w,HPRB}$	water-filled porosity of the HPRB	–
ρ_{HPRB}	bulk density of the HPRB	kg/m^3
ρ_{KMnO4}	particle density of potassium permanganate	kg/m^3
ρ_{MnO2}	particle density of manganese dioxides	kg/m^3
$\rho_{oxidant}$	particle density of the oxidant	kg/m^3
ρ_{sand}	particle density of the sand	kg/m^3

References

Baciocchi, R., D'Aprile, L., Innocenti, I., Massetti, F., Verginelli, I., 2014. Development of technical guidelines for the application of in-situ chemical oxidation to groundwater remediation. J. Clean. Prod. 77, 47–55.

Cha, K.Y., Borden, R.C., 2012. Impact of injection system design on ISCO performance with permanganate-mathematical modeling results. J. Contam. Hydrol. 128 (1–4), 33–46.

Connor, J.A., Bowers, R.L., Paquette, S.M., Newell, C.J., 1997. Soil Attenuation Model for Derivation of Risk-based Soil Remediation Standards. Groundwater Services Inc., Houston, Texas, pp. 1–34.

Crank, J., 1975. The Mathematics of diffusion. Clarendon Press, Oxford.

Crimi, M., Quickel, M., Ko, S., 2009. Enhanced permanganate in situ chemical oxidation through MnO_2 particle stabilization: evaluation in 1-D transport systems. J. Contam. Hydrol. 105 (1), 69–79.

Eklund, B., Beckley, L., Yates, V., McHugh, T.E., 2012. Overview of state approaches to vapor intrusion. Remediat. J. 22 (4), 7–20.

Fischer, M.L., Bentley, A.J., Dunkin, K.A., Hodgson, A.T., Nazaroff, W.W., Sextro, R.G., Daisey, J.M., 1996. Factors affecting indoor air concentrations of volatile organic compounds at a site of subsurface gasoline contamination. Environ. Sci. Technol. 30 (10), 2948–2957.

Hartog, N., Mahmoodlu, M.G., Hassanizadeh, S.M., 2015. Bias by the inappropriate use of the pseudo-first order approach to estimate second-order reaction rate constants: reply to the commentary by Tratnyek (this issue). Sci. Total Environ. 502, 724–725.

Hers, I., Atwater, J., Li, L., Zapf-Gilje, R., 2000. Evaluation of vadose zone biodegradation of BTX vapours. J. Contam. Hydrol. 46 (3–4), 233–264.

Huang, K.C., Hoag, G.E., Chheda, P., Woody, B.A., Dobbs, G.M., 2001. Oxidation of chlorinated ethenes by potassium permanganate: a kinetics study. J. Hazard. Mater. 87 (1–3), 155–169.

ISPRA, 2008. Methodological criteria for absolute risk analysis application at contaminated sites (Italian language), Rome, Italy, March 2008. http://www.isprambiente.gov.it/files/temi/siti-contaminati-02marzo08.pdf (accessed 24.05.16).

ITRC, 2001. Technical and regulatory guidance for in situ chemical oxidation of contaminated soil and groundwater. Interstate Technology and Regulatory Council, In Situ Chemical Oxidation Work Team. http://www.itrcweb.org/Guidance/GetDocument?documentID=44 (accessed 24.05.16).

ITRC, 2007. Vapor intrusion pathway: a practical guideline. Interstate Technology and Regulatory Council, Vapor Intrusion Team, Washington, D.C., January 2007. http://www.itrcweb.org/documents/vi-1.pdf (accessed 24.05.16).

Johnson, P.C., Kemblowski, M.W., Johnson, R.L., 1998. Assessing the significance of subsurface contaminant migration to enclosed spaces. Site-specific alternatives to generic estimates. API Publication 4674. American Petroleum Institute.

Kao, C.M., Huang, K.D., Wang, J.Y., Chen, T.Y., Chien, H.Y., 2008. Application of potassium permanganate as an oxidant for in situ oxidation of trichloroethylene-contaminated groundwater: a laboratory and kinetics study. J. Hazard. Mater. 153 (3), 919–927.

Lahvis, M.A., Hers, I., Davis, R.V., Wright, J., DeVaull, G.E., 2013. Vapor intrusion screening at petroleum UST sites. Ground Water Monit. Remediat. 33 (2), 53–67.

MacKinnon, L.K., Thomson, N.R., 2002. Laboratory-scale in situ chemical oxidation of a perchloroethylene pool using permanganate. J. Contam. Hydrol. 56 (1–2), 49–74.

Mahmoodlu, M.G., Hassanizadeh, S.M., Hartog, N., Raoof, A., 2014a. Oxidation of trichloroethylene, toluene, and ethanol vapors by a partially saturated permeable reactive barrier. J. Contam. Hydrol. 164, 193–208.

Mahmoodlu, M.G., Hassanizadeh, S.M., Hartog, N., 2014b. Evaluation of the kinetic oxidation of aqueous volatile organic compounds by permanganate. Sci. Total Environ. 485-486, 755–763.

Mahmoodlu, M.G., Hassanizadeh, S.M., Hartog, N., Raoof, A., van Genuchten, M.T., 2015. Evaluation of a horizontal permeable reactive barrier for preventing upward diffusion of volatile organic compounds through the unsaturated zone. J. Environ. Manag. 163, 204–213.

McHugh, T., Davis, R., Devaull, G., Hopkins, H., Menatti, J., Peargin, T., 2010. Evaluation of vapor attenuation at petroleum hydrocarbon sites: considerations for site screening and investigation. Soil Sediment Contam. 19 (6), 725–745.

Millington, R.J., Quirk, J.M., 1961. Permeability of porous solids. Trans. Faraday Soc. 57, 1200–1207.

Patterson, B.M., Davis, G.B., 2009. Quantification of vapor intrusion pathways into a slab-on-ground building under varying environmental conditions. Environ. Sci. Technol. 43 (3), 650–656.

Rivett, M.O., Wealthall, G.P., Dearden, R.A., McAlary, T.A., 2011. Review of unsaturated-zone transport and attenuation of volatile organic compound (VOC) plumes leached from shallow source zones. J. Contam. Hydrol. 123 (3–4), 130–156.

U.S.EPA, 2001. Remediation technology cost compendium-year 2000. U.S. Environmental Protection Agency, Office of Solid Waste and Emergency Response, Technology Innovation Office, Washington, DC, EPA 542-R-01-009, September 2001. https://www.epa.gov/sites/production/files/2015-08/documents/542r01009.pdf (accessed 24.05.16).

U.S.EPA, 2004. Memorandum, Interim Measures Cost Compendium. U.S. Environmental Protection Agency U.S. Environmental Protection Agency, Office of Enforcement and Compliance Assurance, Washington, DC 20460 (November 2004. (accessed 23.09.16)).

U.S.EPA, 2015a. OSWER technical guide for assessing and mitigating the vapor intrusion pathway from subsurface vapor sources to indoor air. OSWER publication 9200.2-154. U.S. Environmental Protection Agency, Office of Solid Waste and Emergency Response, June 2015. https://www.epa.gov/sites/production/files/2015-09/documents/oswer-vapor-intrusion-technical-guide-final.pdf (accessed 24.05.16).

U.S.EPA, 2015b. Vapor intrusion screening level calculator, version 3.4. U.S. Environmental Protection Agency, Office of Solid Waste and Emergency Response Vapor Intrusion Assessment. http://www.epa.gov/oswer/vaporintrusion/documents/VISL-Calculator.xlsm (accessed 24.05.16).

U.S.EPA, 2015c. Toxicity and chemical/physical properties for regional screening level (RSL) of chemical contaminants at superfund sites. U.S. Environmental Protection Agency, Region 9, June 2015. http://www.epa.gov/region9/superfund/prg/ (accessed 24.05.16).

Urynowicz, M.A., 2007. In situ chemical oxidation with permanganate: assessing the competitive interactions between target and nontarget compounds. Soil Sediment Contam. 17 (1), 53–62.

Van Genuchten, M.T., 1981. Analytical solutions for chemical transport with simultaneous adsorption. Zero-order production and first-order decay. J. Hydrol. 49 (3–4), 213–233.

Verginelli, I., Baciocchi, R., 2013. Role of natural attenuation in modeling the leaching of contaminants in the risk analysis framework. J. Environ. Manag. 114, 395–403.

Verginelli, I., Baciocchi, R., 2014. Vapor intrusion screening model for the evaluation of risk-based vertical exclusion distances at petroleum contaminated sites. Environ. Sci. Technol. 48 (22), 13263–13272.

Verginelli, I., Yao, Y., Wang, Y., Ma, J., Suuberg, E.M., 2016a. Estimating the oxygenated zone beneath building foundations for petroleum vapor intrusion assessment. J. Hazard. Mater. 312, 84–96.

Verginelli, I., Capobianco, O., Baciocchi, R., 2016b. Role of the source to building lateral separation distance in petroleum vapor intrusion. J. Contam. Hydrol. 189, 58–67.

Waldemer, R.H., Tratnyek, P.G., 2006. Kinetics of contaminant degradation by permanganate. Environ. Sci. Technol. 40 (3), 1055–1061.

Water Security Agency, 2016. Potassium permanganate. Fact sheet WSA 509. http://www.saskh2o.ca/pdf/WSA509.pdf.

Xu, X., Thomson, N.R., 2009. A long-term bench-scale investigation of permanganate consumption by aquifer materials. J. Contam. Hydrol. 110 (3–4), 73–86.

Yan, Y.E., Schwartz, F.W., 1999. Oxidative degradation and kinetics of chlorinated ethylenes by potassium permanganate. J. Contam. Hydrol. 37 (3), 343–365.

Yao, Y., Wu, Y., Wang, Y., Verginelli, I., Zeng, T., Suuberg, E.M., Jiang, L., Wen, Y., Ma, J., 2015. A petroleum vapor intrusion model involving upward advective soil gas flow due to methane generation. Environ. Sci. Technol. 49, 11577–11585.

Yao, Y., Verginelli, I., Suuberg, E.M., 2016. A two-dimensional analytical model of petroleum vapor intrusion. Water Resour. Res. 52 (2), 1528–1539.